Experimental and Numerical Study of the Concrete Stress and Fracture Propagation Processes by Blast

Huaming An, Shun Hou, and Lei Liu*

Abstract—**The dynamic behavior of the concrete by blast is studied by numerical and experimental methods The Holmquist-Johnson-Cook model (HJC) is introduced for modeling the dynamic behavior of concrete. A concrete sample under impact compressive loading during the Hopkinson pressure bar (SHPB) test is modeled to calibrate the Holmquist-Johnson-Cook model. The stress propagation and the stress-strain curves indicate that the HJC model can well represent the dynamic properties of the concrete. Jones-Wilkens-Lee (JWL) equation of state (EOS) then is introduced to model the interaction behavior between the detonation products and the surrounding rock mass. Then stress distribution of the cubic concrete by blast has been obtained and the concrete fracture and fragmentation process has been achieved by experimental study. It is concluded that the HJC model and JWL model together can well model the dynamic behavior of the concrete by blast. The modelled results by blast can well explain the concrete fracture and fragmentation process.**

***Index Terms*—dynamic behavior of concrete, fracture and fragmentation, blast, numerical model**

I. Introduction

Blasting is frequently employed in rock fragmentation, hard rock tunneling and structure demolition. In terms of engineering application, many empirical models or equations has been put forward by some researchers [1-3]. Rossin and Rammler(1993) proposed the Rosin-Rammler equation to characterize the partial-size distribution of material while Kuznetsov (1973) developed a semi-empirical equation for estimation of the size distribution of rock fragments [3, 4]. Kuz-Ram model proposed by Cunningham (1983,1987) is widely used for estimating fragmentation from blasting[1, 5]. Although empirical methods are widely used for engineering purposes, the rock blasting is an extremely complex process and Lack of understanding the complex process of the rock blasting has limited engineers to optimize rock blast design. Thus further research is needed to better understand the fracture and fragmentation process by blast.

Nowadays, numerical methods are wildly employed in the modelling of dynamic rock fracture and fragmentation processes due to the fast development of the computer technology. In terms of hypothesis of materials, there are two main categories of numerical methods, i.e. finite element method and discrete element method. The finite element method is based on the hypothesis of materials continuum. ANSYS-LSDYNA[6], ABAQUS[7, 8], LS-DYNA[9-11] and AUTOYN[12] are the typical finite element method software. Discrete element method is based on the hypotheses that the material is discontinuous.

The repetitive softwares are UDEC[13], DDA[14], DEM [15]There are both advantages and disadvantage for the two kinds of methods. The finite element method is good at modeling the stress distribution and propagation. However, it has difficulty in modeling the fracture and fragmentation of the rock by blast as the method is based on continuous assumptions.

As concrete is widely used as construction material in many engineering projects, e.g. underground excavation projects. In addition, the fast development of the numerical method is widely used in many areas [16-19]. Thus, in this paper, the dynamic behavior of concrete by blast is studied through numerical and experimental methods.

II. Numerical Method

As there are many continuum models for modeling the dynamic behavior of brittle materials, in this section, those models are compared for selecting an appropriate model for modeling the dynamic behavior of concrete by blast.

A. Comparison of the numerical models

In terms of continuum method modeling the dynamic behavior of the brittle material, Holmquist-Johnson-Cook model (HJC), Taylor-Chen-Kuszmaul model (TCK) and Riedel-Thoma-Hiermaier (RTH) are widely used in dynamic behavior modeling [20].

As for the HJC model, most of the important material parameters of concrete have been considered, such as hydrostatic pressure, strain rate, and compressive damage, to describe the compressive damage under large strain and high rate[2]. Thus, the HJC model represents a good compromise between simplicity and accuracy for large-scale computations[20]. Compared with the HJC model, the TCK

Manuscript received January 6, 2019; revised May 23, 2019. This work was supported in part by the Research Start-up Fund for Introduced Talent of Kunming University of Science and Technology (Grant No. KKSY201867017)

Huaming An is with the Faulty Public Security and Emergency Management, Kunming University of Science and Technology, Kunming, China, 650093.

Shun Hou is with the Faculty of Land Resources Engineering, Kunming University of Science and Technology, Kunming, China, 650093.

*Lei Liu is with the Faculty of Land Resources Engineering, Kunming University of Science and Technology, Kunming, China, 650093.Lei Liu is the corresponding author (phone +8615912562467, Email, Huaming.an@yahoo.com)

model considered the tensile stress micro crack density and volume strain and it is capable of characterizing the dynamic fracture of concrete in tension and predicting the brittle tensile failure and the cracking growth of concrete[22]. The RHT model was established on the basis of the HJC model by replacing its porous EOS model with Herrman`s $\mathrm{P}-\alpha$ porous model, and by considering the stress tensor J_3 by building up the yield meridian plane with a cap, different tensile, and compressive meridians [20].

In this research, the HJC model which has been implemented into the finite element code LS-DYNA is used to simulate the dynamic behavior of concrete by blast.

As for the numerical codes used for analyzing the dynamic responses of concrete, Bush (2010) evaluated the accuracy of four analysis codes and five concrete constitute models[23]. Two Lagrangian analysis programs, EPIC and LS-DYNA, as well as Eulerian code, CTH, are compared in his work[23]. The concrete models evaluated in his work includes Holmquist Johnson Cook, Brittle Failure Kinetics, Osborn, Karagozian and Case, and Drucker-Prager[23].Liu et al.(2012) using a three-dimensional finite element code LS-DYNA to simulate the rigid 12.6mm diameter kinetic energy ogive-nosed projectile impact on plain and fiber reinforced concrete [20]. A combined dynamic constitutive model is used to describe the compressive and tensile damage of concrete, which is implemented in the finite element code LS-DYNA [20].

B. HJC model

As the HJC model comprises most of the important material parameters of concrete such as hydrostatic strain, strain rate, and compressive damage, to describe the dynamic behavior of concrete under large strain and high rate[21]. Thus the HJC model was used in this study to simulate the dynamic response of concrete. The model can be expressed in Eq. (1).

$$\sigma^* = \left[A\left(1-D_C\right) + BP^{*N} \right]\left(1+C\ln\left(\dot{\varepsilon}^*\right)\right) \qquad (1)$$

damage, $\sigma^* = \sigma / f_c$ is normalized stress (where f_c is quasi-static uniaxial compressive strength), $P^* = P / f_c$ is normalized pressure (where P is the actual pressure), and $\dot{\varepsilon}^* = \dot{\varepsilon} / \dot{\varepsilon}_0$ is the dimensionless strain rate (where $\dot{\varepsilon}$ is the actual strain rate and $\dot{\varepsilon}_0$ is the reference strain rate).

The HJC model includes three parts, i.e. stress-pressure relationship, the damage model and the equation of state. Fig.1 shows normalized Equation Stress-Normalized Pressure Curve. The equivalent stress, σ^*, and normalized pressure P^* are both normalized by unconfined compressive strength, f_c.

In the model, a damage parameter, D and a cohesive strength constant, A, are proposed. Then, the D is applied to A to represent the difference between undamaged and fractured strength. In figure 1a, B, N, and C are normalized pressure hardening coefficient, exponent, and strain rate constant, respectively. S_{Max} are the normalized maximum strength.

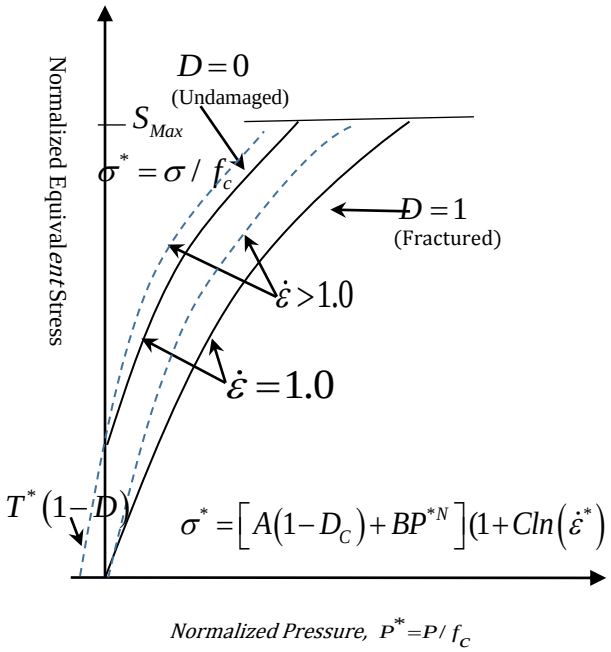

Fig. 1. Normalized Equation Stress-Normalized Pressure Curve

The damage model is illustrated in Fig.2. The model describes the accumulating damage from both the equivalent plastic strain and plastic volumetric strain. The equation can be expressed in Eq. (2) as follows.

$$D = \sum \frac{\Delta\varepsilon_p + \Delta\mu_p}{\varepsilon_p^f + \mu_p^f} \qquad (2)$$

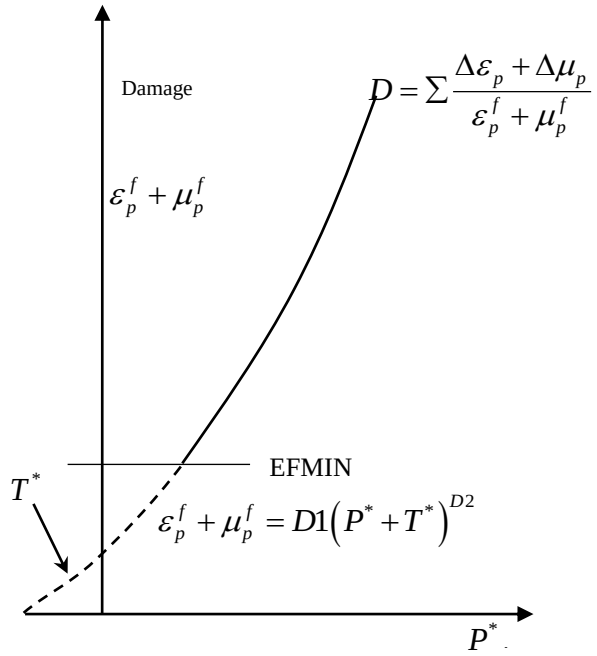

Fig.2. Damage model

In Equation 2, $\Delta\varepsilon_p$ is the equivalent plastic strain while $\Delta\mu_p$ is the plastic volumetric strain. $\varepsilon_p^f + \mu_p^f = f\left(P\right)$ is

the plastic strain to fracture under constant pressure, P. and it can be expressed in Eq.(3)

$$\varepsilon_p^f + \mu_p^f = D1\left(P^* + T^*\right)^{D2} \quad (2)$$

Where D1 and D2 are constants and $P^* = P / f_c$ s normalized pressure (where P is the actual pressure). T^* the normalized maximum tensile hydrostatic pressure.

The Eq.2 and Eq.3 together describe the damage due to the concrete losing its cohesive strength while the air voids collapse.

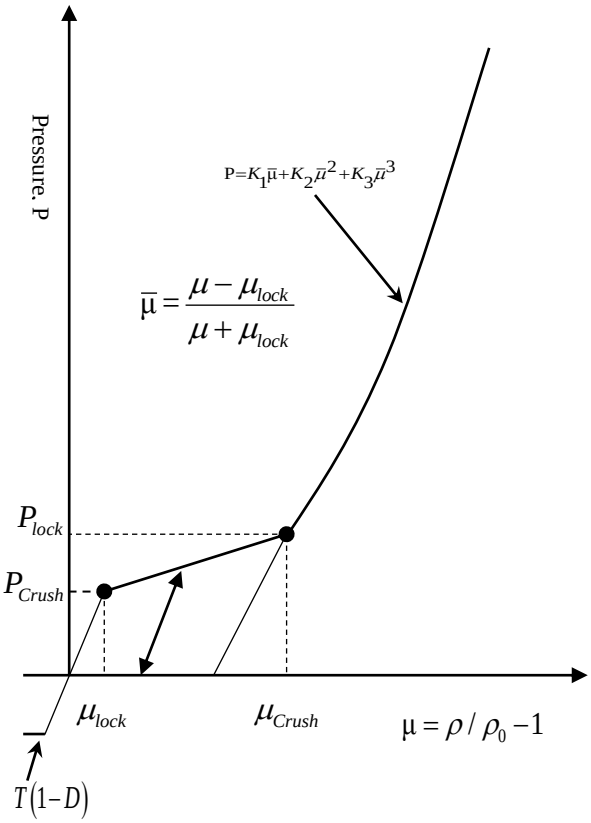

Fig.3. Equation of state

Fig.3 illustrates the hydrostatic pressure-volumetric relationship. The curve can be separated into three response regions. P_{crush} and μ_{crush} are the pressure and volumetric strain which are obtained from uniaxial compression test. T is the maximum tensile hydrostatic pressure.

As shown in Fig.3, the first regions occurs at $P \le P_{crush}$. As can be seen in this section, it is linear elastic region. The second regions occurs at $P_{crush} \le P \le P_{lock}$. This sections is referred to as the transition region. The air voids in the concrete at this regions are gradually compressed out, which results in the plastic volumetric strain. In this region, unloading occurs along the modified path which is interpolated from the adjacent regions[21].

In the third region, all air voids are pressed out of the concrete. At this section, the concrete is fully dense. At this region, the pressure can research P_{lock}, and the relationship can be expressed as follows.

$$P = K_1\bar{\mu} + K_2\bar{\mu}^2 + K_3\bar{\mu}^3 \quad (3)$$

Where $\bar{\mu} = \frac{\mu - \mu_{lock}}{\mu + \mu_{lock}}$, and $\bar{\mu}$ s the modified volumetric strain. The constant K_1 K_2 K_3 are equivalent to those used for concrete with no voids. μ is the standard volumetric strain which can be expressed as $\mu = \rho / \rho_0 - 1$ for current density ρ and initial density ρ_0. μ_{lock}. is the locking volumetric strain and can be expressed as $\mu_{lock} = \rho_{grain} / \rho_0 - 1$ where ρ_{grain} s the grain density.

In terms of tensile pressure, it can be expressed as $P = K_{elastic} \bullet \mu$, $P = K_1 \bullet \mu$ and $P = [(1-F)K_{elastic} + F \bullet K_1] \bullet \mu$ at the elastic region, fully dense region and the transition region respectively. F is the interpolation fact can be expressed as $F = (\mu_{max} - \mu_{crush}) / \left(\mu_{plock} + \mu_{crush}\right)$, where μ_{max} is the maximum volumetric strain and the μ_{plock} s the volumetric strain at P_{lock}.

III. Calibration of HJC Model

The HJC model was calibrated by modelling of the dynamic behavior of concrete during the split Hopkinson pressure bar (SHPB) test.

A. Numerical model

Fig.4 illustrates the numerical model for HSPB test. The concrete sample was placed between the incident bar and the transmission bar. During the test, four half SINE stress waves with the peak values of 80MPa, 100MPa, 120MPa, 150MPa, are applied on the incident bar to simulate the dynamic behaviour of concrete under various loading rates.

Table 1 shows the parameters for the incident bar and the transmission bar while the table lists the parameters for concrete sample.

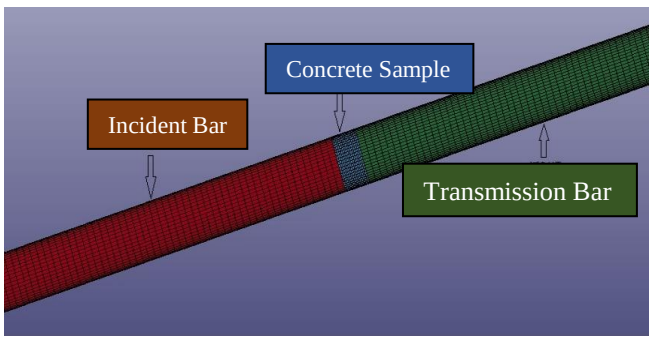

Fig.4. Numerical model of rock sample placed between incident and transmission bar

TABLE 1. PARAMETERS OF THE NUMERICAL MODEL FOR INCIDENT BAR TO TRANSMISSION BAR

D/mm	L/mm	E/GPa	ρ/kg/m^3	μ
75	2000	211	7795	0.285

B. *Modeled result*

Fig.5 shows the stress-strain curves for the concrete under various strain rates. The stress strain curve with the strain rate of 149/s is taken as an example. It is obvious that the curve includes three regions: a linear-elastic deformation region, a non-linear deformation region and a post-failure region. Thus, although the concrete experiences a high strain rate loading, it still indicant a typical brittle material failure process. Comparison of the curves with different loading rates can indicates that the loading rate significantly influent the concrete strength.

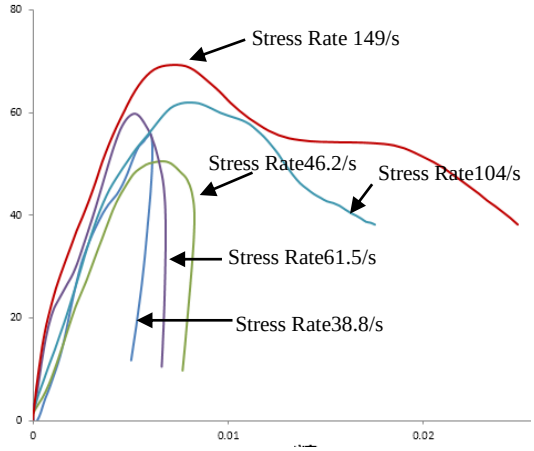

Fig.5 Stress curves for concrete under various strain rates

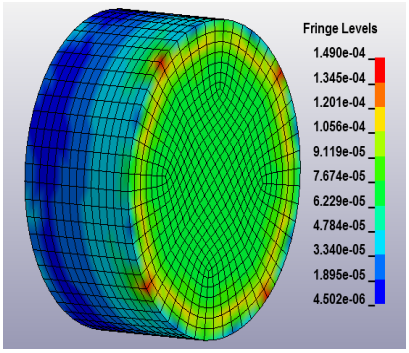

(a) 398μs

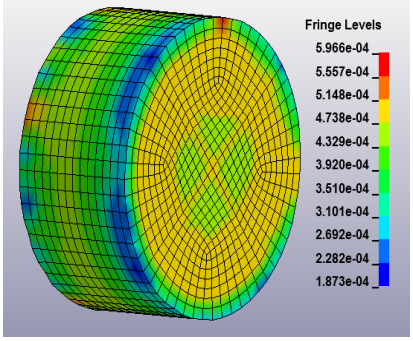

(b)530μs

Fig.6 Stress distributions at different time during the SHPB test

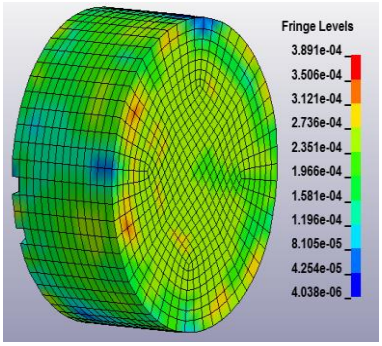

(c) 662μs

Fig.6 Stress distributions at different time during the SHPB test (continued)

Initially, the stress concentration appeared at the contact surface between the specimen and the incident bar as illustrated in Fig.6 at 398 μs . Then it propagates to another contact surface of the specimen and the transmission bar as illustrated in Fig.6 at 530 μs the stress concentration reaches the dynamic strength of the concrete, the cracks are produced as illustrates in Fig.6 at 662μs.

The stress-strain curves and the stress propagation process indicates the HJC model can well represent the dynamic properties of concrete.

IV. NUMERICAL MODELLING OF THE DYNAMIC BEHAVIOR OF CONCRETE BY BLAST

A. *Equation of state for explosive dynamic loads*

It is essential to model the interaction behaviour between the detonation products and the surrounding rock mass while modelling the dynamic behaviour of concrete by blast. The generated pressure-time histories from the empirical equations are commonly used for most of numerical modelling of the rock blasting. However, the equation has many limitations and uses various crude approximations: e.g. it does not take into account any confinement, the shape of the explosive charge, shadowing by intervening objects, and so on[7]. In this study, the Jones-Wilkens-Lee (JWL) equation of state (EOS) is used to model interaction behaviour between the detonation products and the surrounding rock mass.

Eq. 4. is the JWL equations of the state, which contains parameters describing the relationship among the volume, energy and pressure of detonation products.

$$P = A\left(1-\frac{w\rho}{R_1\rho_0}\right)\exp\left(-R_1\frac{\rho_0}{\rho}\right)+B\left(1-\frac{w\rho}{R_2\rho_0}\right)\exp\left(-R_2\frac{\rho_0}{\rho}\right)+\frac{w\rho^2}{\rho_0}E_{m0} \tag{4}$$

Where P is the pressure, A， B， R1， R2 and ω are material constants, ρ_0 and ρ are the densities of the explosive and the detonation products, respectively.

The Parameters for Eq.4 in this research can be found in Table 2.

TABLE 2 TNT EXPLOSIVE PARAMETERS

A/GPa	B/GPa	R_1	R_2	ω
540.9	9.4	4.5	1.1	0.35
E_0/GJ·m^{-3}	V_0	D/m·s^{-1}	P_{CJ}/GPa	ρ/kg·s^{-3}
8	1.0	6718	18.5	1630

B. Numerical model

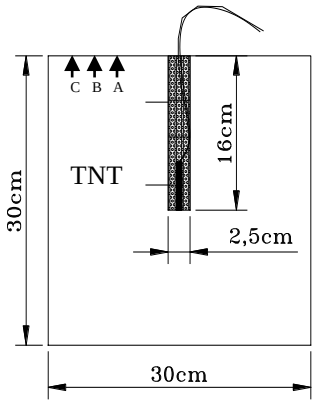

(a) Geometrical model

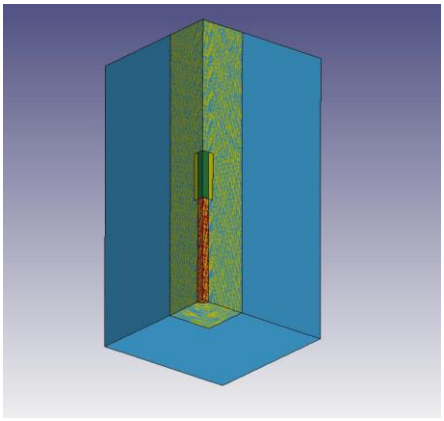

(b) Numerical model

Fig.7 Geometrical and numerical model

Fig.7 illustrates the geometrical model and the numerical model for the simulation of blasting. As shown in the Fig.7a, a cubic model with 30cm in length is used and a borehole with 16cm deep and 2.5cm in diameter is set at the centre of the model. As shown in Fig.7b, only a quarter of the numerical model is model in order to save the computational resource.

C. Stress distribution during blasting

Fig.8 illustrates the stress distribution at different times. Initially, the stress was produced around the borehole while the explosive was detonated as illustrated in Fig.8a. Then the stress propagated to the boundaries of the specimen. Fig.8b shows that the stress reached the boundaries. Due to the continuum assumption for the numerical model in the finite element method, the specimen cannot be separated into fragments during the blast. However, as the stress reaches the boundaries, the stress will be reflected and the compressive stress turns into tensile stress. As well known, the tensile strength of the concrete is much smaller than the compressive strength. Thus, the tensile failure will occur at the boundaries of the concrete model. In addition, as the initial compressive stress at the borehole is much higher than the compressive strength, compressive failure also occurs around the borehole. The concrete sample is supposed to be separated into many fragments.

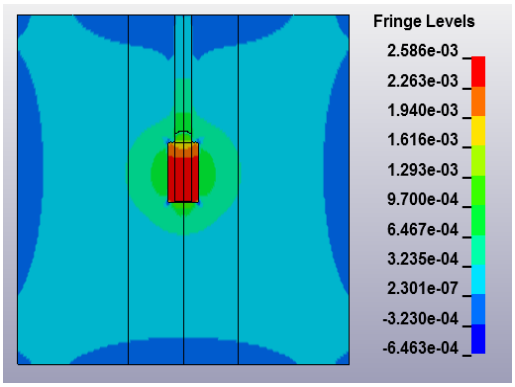

（a）470μs

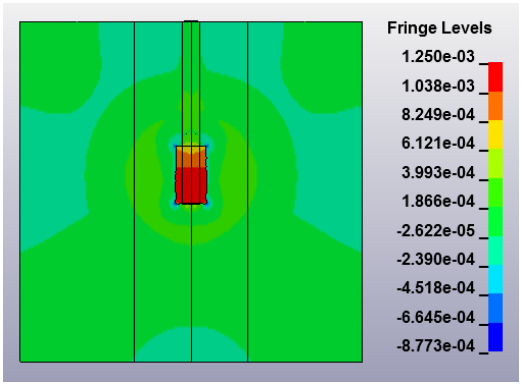

（b）1882μs

Fig.8 stress distribution during blasting

Fig.9 shows the pressure-time curves at Point A and B while Fig.10 shows the pressure-time curves at Point at point C.

As the speed of the stress wave is about 5500m/s, it almost reaches at Point A and Point B at the same time. The stresses at the point begin to increase. As can be seen in Fig.9, the peak stress at Point A is much higher than that at Point B as A is much closer to the borehole. As the stresses meet their peak values, the stresses begin to decrease. As shown in Fig.10, it takes a while for the stress wave reaches Point C. Thus initially, there are no stress at Point C. Then stress at Point C begin to increase sharply. The peak stress is much smaller than that at Point B and A as the stress attenuates while it propagate from the borehole to the boundaries. After the stress at Point C reach its peak value, it drops quickly. Finally, the stress decrease to zero as the concrete is blasted into fragments.

The stress-time curves indicates a typical brittle failure process. It includes three regions: a linear-elastic deformation region, a non-linear deformation region and a post-failure region.

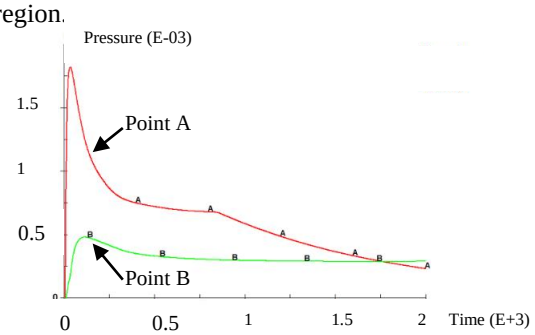

Fig. 9 Pressure-time curve for point A and B

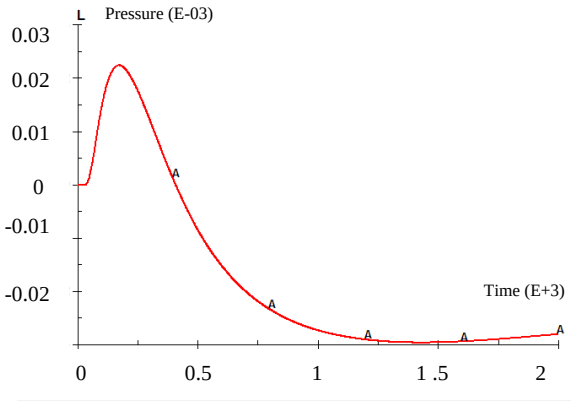

Fig. 10. Pressure-time curve for point C

V. Experimental Study the Concrete Fracture and Fragmentation Process by Blast

An experimental test was conducted to study the concrete fracture and fragmentation process. As shown in Fig. 11. The cubic concrete was made with the height of 30cm. A borehole was drilled at the centre of the top surface. The borehole is 16cm in depth and 2.5cm in width. The concrete sample is made as the same as the numerical model. 5 gram of TNT explosive was put the end of the borehole.

Fig. 11 Cubic concrete with a borehole at the centre of the top surface

As mentioned in numerical modelling (Fig.8), the stress initiate at the borehole and propagate around the borehole wall to the boundaries of the concrete model. Thus, there are no cracks or fragments can be seen at the outside of the concrete as shown in Fig.12a.

While the stress reached the boundaries of the cubic sample, tensile stress was produced. Thus tensile failure can be seen at the surface of the concrete as shown in Fig.12b. Meanwhile, the high pressure gas was also produced while the explosive was detonated. The gas pressure also plays an important role. The high pressure gas flow through the fracture and help the fracture propagate (Fig.12b). Thus, more fracture can be seen. Then fragments also can be threw away by the high pressure as (Fig.12c). Finally, the concrete sample was blast into pieces due to the compressive stress wave, the produced tensile stress and the high pressure gas (Fig.12d~i).

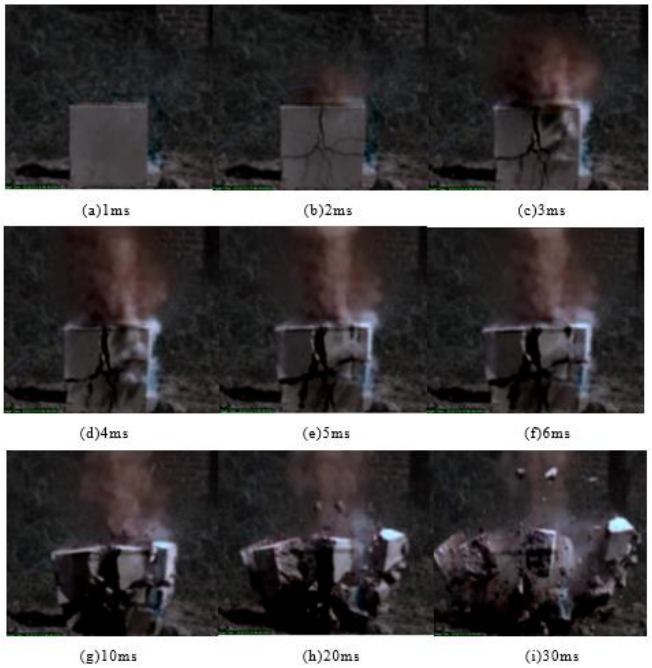

Fig. 12. Concrete fracture and fragmentation process by blast

VI. Conclusion

In this study, the experimental and numerical modeling of the concrete like material is reviewed. The Holmquist-Johnson-Cook model (HJC) for modelling of the concrete behavior under dynamic loads was introduced in details. The HJC model was calibrated by modelling of the concrete dynamic test by Hopkinson pressure bar (SHPB). The stress propagation during the SHPB test for the concrete sample was obtained, the stress-strain curves was also achieved. The stress-strain curves indicates a typical brittle material failure process. The dynamic behavior of the concrete modelled using the HJC model indicates that the HJC model can well represent the brittle material in terms of the dynamic properties. Then the HJC model which implemented into the finite element method was used to study the concrete dynamic behavior by blast. In addition, the Jones-Wilkens-Lee (JWL) equation of state (EOS) is used to model interaction behaviour between the detonation products and the surrounding rock mass. The stress distribution at different times were obtained and the pressure-time curves at different times are described. In order to study the concrete fracture and fragmentation process by blast, the experimental study was conducted. The numerical method and experimental method together show the stress propagation and the fracture and fragmentation process. It is conduced that:

- The HJC model which implemented into LS-DYNA can model the concrete behavior under impact loads.
- The stress-strain curves under various loading rates illustrate a typical brittle material failure process and the comparison of those curves under various loading rates indicates that the compressive strength of the concrete increases with the loading rate.

- The HJC model for the concrete material and the JWL model for the explosive together can well model the dynamic behaviour of the concrete by blast.
- The numerical and experimental study well illustrate the stress propagation process and the concrete fracture and fragmentation process.

VII. Acknowledgements

The research presented is supported by Research Start-up Fund for Talent of Kunming University of Science and Technology, Grant No. KKSY201867017), which is greatly appreciated. Moreover, the authors would like to thank the anonymous reviewers for their valuable comments and constructive suggestions.

References

[1] Cunningham, C. Fragmentation estimations and the Kuz-Ram model-Four years on. in Proc. 2nd Int. Symp. on Rock Fragmentation by Blasting. 1987.
[2] Kisslinger, C., The generation of the primary seismic signal by a contained explosion. 1963, DTIC Document.
[3] Kuznetsov, V., The mean diameter of the fragments formed by blasting rock. Journal of Mining Science, 1973. 9(2): p. 144-148.
[4] Rossin, P. and B. Rammler, The Laws Governing the Fineness of Powdered Coal. Inst. Of Fuel, 1933: p. 29-36.
[5] Cunningham, C. The Kuz-Ram model for prediction of fragmentation from blasting. in Proceedings of the first international symposium on rock fragmentation by blasting, Lulea, Sweden. 1983.
[6] Wei, X., Z. Zhao, and J. Gu, Numerical simulations of rock mass damage induced by underground explosion. International Journal of Rock Mechanics and Mining Sciences, 2009. 46(7): p. 1206-1213.
[7] Liu, H., et al. Numerical procedure for modelling dynamic fracture of rock by blasting. in Controlling Seismic Hazard and Sustainable Development of Deep Mines: 7th International Symposium On Rockburst and Seismicity in Mines (rasim7), Vol 1 and 2. 2009. Rinton Press.
[8] Saharan, M.R. and H. Mitri, Numerical procedure for dynamic simulation of discrete fractures due to blasting. Rock mechanics and rock engineering, 2008. 41(5): p. 641-670.
[9] Ma, G. and X. An, Numerical simulation of blasting-induced rock fractures. International Journal of Rock Mechanics and Mining Sciences, 2008. 45(6): p. 966-975.
[10] Wang, Z.-L., Y.-C. Li, and R. Shen, Numerical simulation of tensile damage and blast crater in brittle rock due to underground explosion. International Journal of Rock Mechanics and Mining Sciences, 2007. 44(5): p. 730-738.
[11] Wang, Z., Y. Li, and J. Wang, A method for evaluating dynamic tensile damage of rock. Engineering fracture mechanics, 2008. 75(10): p. 2812-2825.
[12] Zhu, Z., B. Mohanty, and H. Xie, Numerical investigation of blasting-induced crack initiation and propagation in rocks. International Journal of Rock Mechanics and Mining Sciences, 2007. 44(3): p. 412-424.
[13] Zhao, X., et al., UDEC modelling on wave propagation across fractured rock masses. Computers and Geotechnics, 2008. 35(1): p. 97-104.
[14] Ning, Y., et al., Modelling rock fracturing and blast-induced rock mass failure via advanced discretisation within the discontinuous deformation analysis framework. Computers and Geotechnics, 2011. 38(1): p. 40-49.
[15] Fakhimi, A. and M. Lanari, DEM–SPH simulation of rock blasting. Computers and Geotechnics, 2014. 55: p. 158-164.
[16] Hollis, L., et al., Finite element analysis to compare the accuracy of the direct and mdev inversion algorithms in MR elastography. IAENG Int J Comput Sci, 2016. 43(2): p. 137-146.
[17] Sun, T. and R. Zheng, An Upwind-mixed Finite Element Method with Moving Grids for Quasi-nonlinear Sobolev Equations. International Journal of Applied Mathematics, 2017. 47(4):P. 465-470.
[18] Zeng, Y., et al., Analysis on Time-frequency Characteristics and Delay Time Identification for Blasting Vibration Signal by Hilbert-Huang Transform in Fangchenggang Nuclear Power Station. Engineering Letters, 2017. 25(3): P. 329-335.
[19] Zhou, J., et al., The Analysis of Blasting Seismic Wave Passing Through Cavity Based on SPH-FEM Coupling Method. Engineering Letters, 2019. 27(1):P.114-119.
[20] Lu, G., X. Li, and K. Wang, A numerical study on the damage of projectile impact on concrete targets. Computers & Concrete, 2012. 9(1): p. 21-33.
[21] Holqmuist, T., G. Johnson, and W. Cook. A computational constitutive model for concrete subjected to large strains, high strain rate, and high pressures. in 14th international symposium on ballistics. 1993.
[22] Taylor, L.M., E.-P. Chen, and J.S. Kuszmaul, Microcrack-induced damage accumulation in brittle rock under dynamic loading. Computer methods in applied mechanics and engineering, 1986. 55(3): p. 301-320.
[23] Bush, B.M., Analytical evaluation of concrete penetration modeling techniques. 2010.